Journal of Archaeological Science: Reports 26 (2019) 101910

Contents lists available at ScienceDirect

Journal of Archaeological Science: Reports

journal homepage: www.elsevier.com/locate/jasrep

The sacred canals of the Temple of Bastet at Bubastis (Egypt): New findings from geomorphological investigations and Electrical Resistivity Tomography (ERT)

Eva Lange-Athinodorou[a,*], Amr Abd El-Raouf[b,c,**], Tobias Ullmann[d], Julian Trappe[d], Julia Meister[d], Roland Baumhauer[d]

[a] Institute of Egyptology, University of Würzburg, Residenzplatz 2, Tor A, 97070 Würzburg, Germany
[b] School of Earth Sciences, Zhejiang University, Zheda Road 38, Hangzhou 310027, China
[c] Geology Department, Faculty of Science, Zagazig University, Zagazig 44519, Egypt
[d] Institute of Geography und Geology, Department of Physical Geography, University of Würzburg, Am Hubland, 97074 Würzburg, Germany

ARTICLE INFO

Keywords:
Tell Basta
Nile Delta
Herodotus
Sacred Lakes
Isheru

ABSTRACT

This contribution highlights recent findings of geomorphological and geophysical investigations that were undertaken at the excavation site of Bubastis (Eastern Nile Delta, Egypt) in order to find evidence of the existence and location of the sacred canals of Bubastis that were described by Herodotus in the 5th century BCE. None of the preceding archaeological missions have reported remains of these canals. Drilling and sediment analyses in 2018 revealed clayey/silty deposits in the centre of the site at depths below 2.5 m above sea level, close to the northern enclosure of the Temple of Bastet. The recovered sediments, with a thickness of at least four metres, were situated below the floor level of the Temple of Bastet of the 1st mill. BCE and contained fragments of pottery as well. Conducted DCR (direct current resistivity) and 2D electrical surveying confirmed the drilling results. These geophysical investigations indicated trench-formed layers of low resistivity values adjunct to the northern enclosure of the Temple of Bastet. The recovered deposits were therefore interpreted as infills that were most likely accumulated in a fluvial system of very low energy, e.g. an ox-bow lake, (abandoned) channel or lake. Presumptively, this waterway was prone to refilling, but also to infilling, by a tributary situated north or north-west of the Temples of Bastet and Pepi I.

1. Introduction

In urban contexts, ancient Egyptian temples were the most vital parts of cities. As temples were not only centres of religious and cultic significance, but were also of economic and administrative importance, the evolution of a city was always connected to the presence of temples and other cult installations of one or more local deities over many centuries (Bussmann, 2010; Léclere, 2008). In addition to being essential elements of cities and settlements in the ways described above, temple areas (i.e. the *temenos*) were thought to be the residences of deities. They were most sacred and needed to be singled out from other urban districts not only by the use of specific architecture that emphasized their importance, but by a multitude of other elements as well, as dictated by the requirements of the daily cultic activity.

Therefore, a Temenos usually contained much more than just the main temple building itself: the annex temples of associated cults, buildings for the priesthood and other serving personnel of the cult, buildings of administrative or economic use, such as magazines, offices and archives, workshops and sometimes even areas for the keeping and breeding of sacred animals related to the cult of the deity in question, all surrounded by a more or less massive enclosure wall (Assmann, 1984; Arnold, 1992; Wilkinson, 2000; Wilson, 2010).

A very specific feature of such temples was the so-called sacred lakes, the *Isheru* of the ancient Egyptian texts. Sacred lakes provided water for all kinds of purifying rites and activities. More importantly, however, a core element of many religious temple festivals, the rowing of the sacred barque of the deity, took place on the sacred lake. As we can deduce from the written sources, sacred lakes were specifically associated with the temples of goddesses who would appear as lionesses, specifically Sekhmet, Mut, Wadjet and Bastet, to name but a few

* Corresponding author.
** Correspondence to: A. A. El-Raouf, School of Earth Sciences, Zhejiang University, Zheda Road 38, Hangzhou 310027, China.
E-mail addresses: eva.lange@uni-wuerzburg.de (E. Lange-Athinodorou), amr_abdelraouf@zu.edu.eg (A.A. El-Raouf).

https://doi.org/10.1016/j.jasrep.2019.101910
Received 19 December 2018; Received in revised form 14 June 2019; Accepted 22 June 2019
Available online 27 June 2019

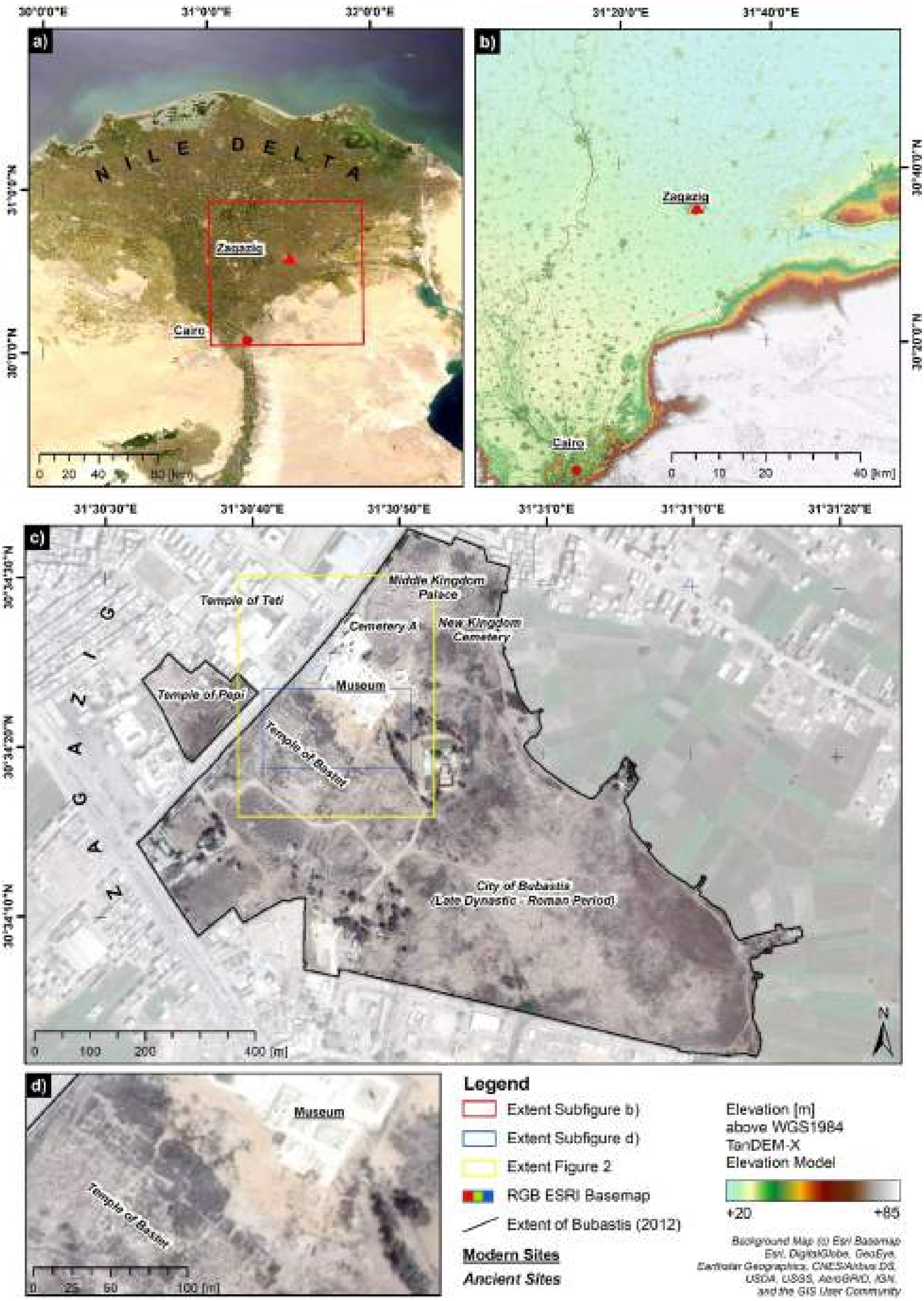

(caption on next page)

Fig. 1. Overview and location of the study area and the current extent of Bubastis: a) Terra MODIS True Color Corrected Reflectance from 13 May 2019 (© *earthdata.nasa.gov*), b) Digital Elevation model of the TanDEM-X Mission (©DLR, 2012), c) current extent of Bubastis, ancient and modern features, d) enlargement of the focus area between the Temple of Bastet and the modern museum. *Background Maps © Esri Basemap*.

(Yoyotte, 1962; Sauneron, 1983; Geßler-Löhr, 1983; Tillier, 2010).

Lioness goddesses were considered mighty and fierce, and always possessed a dangerous and unpredictable aspect. In ancient Egyptian mythology, they were connected to the sun god Ra, bearing the epithet "Daughter of Ra" or "Eye of Ra". The presence of a cooling body of water, ideally surrounding her temple, was thought to calm and please the fiery temperament of such a goddess while shielding the people in the cities from her potential rages at the same time (Tillier, 2010; Lange-Athinodorou, 2019). Interestingly, the ancient Egyptian term *Isheru* generally designates lakes of a particular horseshoe shape. The origin of this specific form is unknown; however, one could look at natural prototypes, such as the lakes that emerged on the estuaries of the Wadis after rainfall, when the remaining water would accumulate with sediments in a fan-like shape after flowing out of the Wadi (Sauneron, 1963-64). Obviously, such lakes would attract wildlife and thereby provide very suitable hunting grounds for lions, thus creating a connection between crescent-shaped lakes and lionesses. Even though ancient sources witness to the presence of such sacred lakes and waterways, actual physical records and archaeological proof of their existence are still very rare. One reason for this is that such features are now silted up and have disappeared from the surface.

Besides traditional approaches that concentrated on the analyses of known artificial water basins lined with stone slabs, e.g. in the Amun Temple at Karnak in the Nile Valley or Tanis in the Nile Delta (Montet, 1966; Geßler-Löhr, 1983; Brissaud, 2018), recently new methods have also been applied to reconstruct the environmental setting of a site, i.e. to prospect and detect buried ancient waterways. Especially, geophysical methods (e.g. direct current (DC) resistivity, ground penetrating radar, seismic refraction) have become increasingly important as non-invasive, non-destructive, rapid and cost-effective approaches (Patella and Hesse, 1999; Simms and Albertson, 2000; Bevan and Roosevelt, 2003; Bates et al., 2007; Deiana et al., 2018). Among these methods, DC resistivity surveying in the form of DCR (direct current resistivity) sounding and Electrical Resistivity Tomography (ERT) are promising means of delineating sedimentological differences of the subsurface without soil disturbance (e.g. Maillet et al., 2005; Torrese et al., 2013; El-Kenawy et al., 2013; Kasprzak and Traczyk, 2014; Nimnate et al., 2017; Toonen et al., 2017). A recent study applying these methods was provided by Rowland and Strutt (2011) conducted at Quesna and Kom el-Ahmar (Markaz Minuf) in the Nile Delta. The authors reported the ERT technique to be suited for detecting changes in the site deposits by noting substantial differences in electrical resistivity: massive silty clay sediments, which were found in the drill core data, were at the same time indicated by very low resistivity values in the ERT.

This study presents a similar approach that combines geoelectrical measurements (i.e. DCR sounding and ERT) and geomorphological investigations (i.e. drilling and sediment analyses) in order to detect sedimentary layers of ancient waterways at the ancient site of Bubastis (Tell Basta) in the immediate surroundings of the Temple of Bastet. The investigations were undertaken in 2016 and 2018 with the objective of finding evidence on the existence and location of the sacred canals of the Temple of Bastet as mentioned in ancient Egyptian texts and described by Herodotus. Even though the site has been the subject of several archaeological missions since the late 19th century, no findings nor physical records of these sacred canals have been reported yet: there is so far no proof of the existence of the canals of Bubastis.

2. Study area

By at least the 6th millennium BCE, two main branches of the Nile, i.e. the Pelusiac and the Tanitic branch, crossed the southeastern Nile Delta (Pennington et al., 2017). While convincing reconstructions of the course of the Pelusiac branch exist (Butzer, 1976; Bietak, 1975; Said, 1993; Butzer, 2002), the course of the Tanitic branch remains less clear (Bietak, 1975; Ullmann et al., 2019). The important role of these river branches for the evolution, historical development and continuance of settlements in the Nile Delta is well known (Bietak, 1975). The location of settlements was always clearly connected to the changing course of the waterways (Bietak, 1975) and to the underlying geology, i.e. location of local *Gezira* (Arabic for "island") mounds and/or levee systems (Butzer, 1959; Said, 1981; Said, 1993). Judging from the archaeological record, the Pelusiac branch played an especially major role in the southeastern Delta, as the remains of numerous settlements mainly dating into the period from the second half of the 3rd millennium BCE until the time of the Roman emperors have been found on its banks, outnumbering the remains of settlements located on the Tanitic branch from the time of the late 3rd millennium BCE onwards (Bietak, 1975).

The main city of the southeastern Nile Delta, Bubastis, benefited from its location close to the efficient Pelusiac branch (Bietak, 1975; Bietak and Lange, 2014; Bakr and Lange, 2016). Bubastis was of outstanding cultural and political importance from the Predynastic Period (late 4th mill. BCE) to its decline in the time of the Roman dominion. It even served as the capital or residential city of the Libyan kings of the 22nd dynasty in the 1st mill. BCE (Kitchen, 1996; Lange, 2008; Lange, 2010). Today, the excavation site of Bubastis (Tell Basta) is located at the southeastern city border of Zagazig (Fig. 1), the capital of the Egyptian province Sharqiya.

Since the late 19th century, the site has been the subject of archaeological investigations, e.g. Naville, 1891; Habachi, 1957; Farid, 1964; El-Sawi, 1979; van Siclen, 1991; Bietak and Lange, 2014; Lange, 2006; Lange, 2009; Lange, 2013; Lange, 2015; Lange and Ullmann, 2015; Bakr and Lange, 2016, which have focused mainly on the ancient remains in the northern and central part of the site, i.e. the Temple of Bastet (925–343 BCE), the temples of Teti and Pepi I (Old Kingdom 2300–2250 BCE), the Middle Kingdom Palace (1875–1820 BCE) and the Old, Middle and New Kingdom Cemeteries (2300–1000 BCE). However, large parts of the site are still unexplored today, especially the southern part of the tell, or have become inaccessible due to the urban development of Zagazig (Lange et al., 2016). Therefore, it is difficult to gain a complete picture of the structure of the ancient city, its full extent, its hydrogeographical and geomorphological context.

Notably, Herodotus (5th century BCE) provided a description of the Temple of Bastet and the centre of the city:

> "*Other Egyptian towns, to my thinking, were so dealt with, but the level of Bubastis was raised more than any. In this town there is a Temple of Bubastis, and it is a building most worthy of note. Other temples are greater and more costly, but none pleasanter to the eye than this. Now Bubastis in the Hellenic tongue is Artemis, and her temple is ordered thus: Except the entrance it is completely surrounded by water; for channels come in from the Nile, not joining one another, but each extending as far as the entrance of the temple, one flowing round on the one side and the other on the other side, each a hundred feet (approx. 30 m) wide and shaded over with trees; and the gateway has a height of ten fathoms, and it is adorned with figures six cubits high, very noteworthy. This temple is in the middle of the city and is looked down upon from all sides as one goes round, for since the city has been banked up to a height, while the temple has not been moved from the place where it was at the first built, it is possible to look down into it: and round it runs a stone wall with figures carved upon it, while within it there is a grove of very large trees planted round a large temple-house, within which is the image of the goddess: and the breadth and length of the temple is a furlong every way. Opposite the entrance there is a road paved with stone for about three furlongs, which*

leads through the market-place towards the East, with a breadth of about four hundred feet; and on this side and on that grow trees of height reaching to heaven: and the road leads to the Temple of Hermes." (Herodotus ii. 137–138).

Apart from the description of Herodotus mentioned above, a number of ancient Egyptian texts refer to the sacred canals of Bastet, albeit rather vaguely. Thus Papyrus Brooklyn 47.218.84 (second half of the 7th century BCE) contains a compendium of local myths of the cities of the Nile Delta and describes the statue of Bastet in her temple as follows: "(…) *An image of the water surrounds her completely*. *The length of 7* […]" (Meeks, 2006, 20 § 21 [IX.3-IX.5]; Lange et al., 2016). The same papyrus contains a description of her appearing in her sacred barque as well: "*Her navigation was made* (…) *on the Isheru* (…)" (Meeks, 2006, 20 § 22 [IX.6-IX.8]; Lange et al., 2016). Furthermore, an inscription on the eastern wall of the Ptolemaic enclosure wall of the Temple of Horus at Edfu refers to the same feature: "*Bastet*, *the Great One*, *lady of Bubastis* (…) *under* (*whose temple*) *the Nile flows*" (Lange et al., 2016).

The above-mentioned texts hint at the obvious significance of the canals. Most fascinating is the fact that, in this case, the waterways seem to originate from a preexisting feature of the landscape, like an oxbow lake or an abandoned channel. Such features would be prone to refilling, but also to infilling.

To find evidence of the sacred waterways, six drillings were carried out in the northern part of the excavation area (among other locations like A2, A3, B1, B2; see Fig. 2) in March 2016. Even though the sediment analyses proved the existence of underlying Gezira sands, i.e. the Temple of Bastet, the Middle Kingdom Palace and the New Kingdom Cemetery are situated on a Gezira (Ullmann et al., 2019; see Fig. 3), no physical records on the existence of the canals of the Temple of Bastet were discovered.

3. Material and methods

3.1. Drillings and sediment analyses

Another survey in March 2018 continued the investigations of 2016 by adding seven drillings of different depths (Z1, Z2, Z3, Z4, Z5; for drilling locations 2016 & 2018 see Figs. 2 & 3), aiming to get new insights on the environmental history and the location of the temple canals. The drilling locations Z1-Z5 are situated in the area between the northeastern border of the Temple of Bastet and the site museum. As in 2016, the manually operated Edelman drill bucket auger was used to minimize disturbance of the site. The maximum depth reached was approximately seven metres. The terrain surface elevation was measured with optical levelling equipment (Leica TS06) and the depth of the sampling was estimated using a measuring tape. All depths refer to the local system that is used to document the excavations, i.e. the entrance of the Temple of Bastet is located at 3.35 m above sea level (asl). The sediment samples were described and analysed on site, following BKA (2005) and FAO (2015), and no further laboratory analyses were performed. The dominating grain sizes, the sediment colour, as well as the presence of redoximorphic features and anthropogenic artefacts (potsherds and charcoal fragments) were documented for each sample.

The equipment allowed for fast drilling progress but generated mixed sediment samples. Additionally, the approach limits the interpretability of the samples, as sedimentary structures are usually destroyed during drilling. The groundwater table usually marked the maximum depth that could be reached using the Edelman equipment, due to the mixing of water and sediment. In addition, fragments larger than the drill head opening could not be passed. The drilling locations were documented using a standard GPS device (Garmin GPSMAP 60CSx).

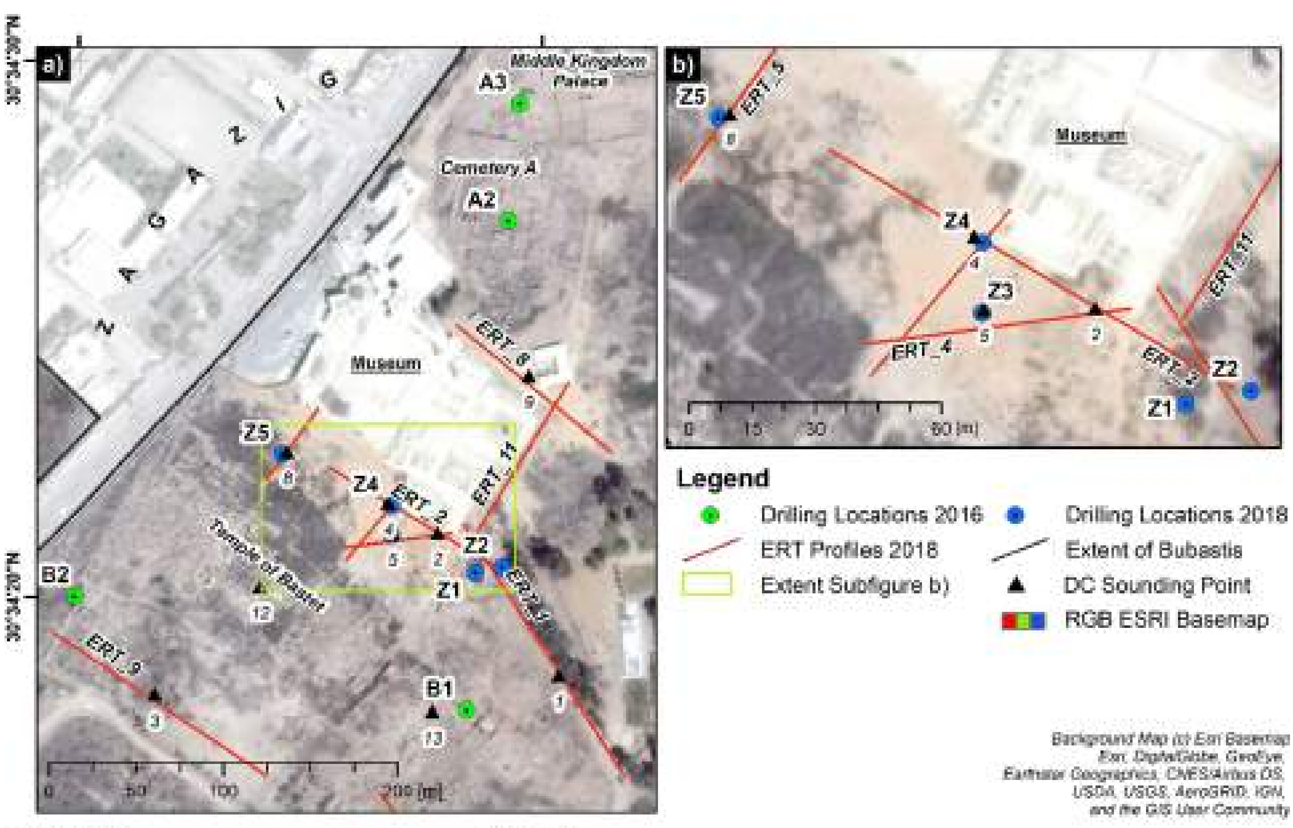

Fig. 2. Overview of drilling locations (2016 & 2018) and the position of 2D Electrical Resistivity Tomography (ERT) profiles (2018): a) drilling locations, DCR sounding points and ERT profiles in the central area of Bubastis between the Temple of Bastet and the site museum, b) enlargement of the focus area between the northern border of the Temple of Bastet and the museum. *Background Map© Esri Basemap*.

Fig. 3. Overview of drilling locations (2016 & 2018) and examples of sediment samples: a) panoramic overview of the excavation area and approximate location of the drilling locations, b) image of the Temple of Bastet, c) drilling in spring 2018 at borehole Z3, d) sediment sample "Surface Layer" taken at borehole Z3 in spring 2018 from a depth of 5.5 m asl, e) sediment sample "Gezira Sand" taken at borehole B1 in 2016 at 1.5 m asl seen through a magnifying glass, f) sediment sample "Silt and Clay Layer" taken in 2018 at borehole Z3 from a depth of 1.5 m asl. *Images taken by T. Ullmann in 2015, 2016 & 2018.*

3.2. Direct current resistivity (DCR) and Electrical Resistivity Tomography (ERT)

In 2018 DCR soundings and ERT measurements were conducted parallel to the drilling (for locations of DCR sounding points and ERT profiles see Fig. 2). These techniques aim to image the spatial distribution of the apparent electrical resistivity in the underground for single points (1D) or along survey lines (2D). The electrical resistivity values of sedimentary layers are, among other factors (e.g. temperature, pH-value etc.), dependent on the soil water content and the grain size. Fine-grained sedimentary layers (e.g. dominated by silt and clay) frequently show lower resistivity values than coarse-grained layers (e.g. dominated by sand and pebbles) (Tellford et al., 1990; Reynolds, 2011). Moreover, higher soil moisture usually favors lower electrical resistivity (Rowland and Strutt, 2011). However, the relation of the measured electrical resistivity values and the properties of the sedimentary layers is very site-specific and thus ambiguous in most cases (Tellford et al., 1990; Reynolds, 2011). A meaningful interpretation of ERT and DCR measurements therefore essentially needs to be backed up by physical sedimentary records, i.e. from drilling.

The geophysical field survey was executed in gradual stages. The DCR soundings were measured to determine the distribution of the subsurface layers. According to the results, some localities were chosen for 2D ERT profiling. The joint implementation of these methods is necessary in order to enhance the resolution of the survey, as each method presents different sensitivity and resolution, according to the physical properties of different materials.

A total of 13 DCR sounding points were measured to cover most of the area in the central locale of Bubastis between the Temple of Bastet and the museum. The electrical soundings were carried out using Schlumberger array with maximum current spacing (AB) of 140 m. According to the available boreholes and geological and archaeological information, the applied spreading is long enough to reach the depth of the buried Gezira. Because the electrical resistivity of sediments depends on lithology, water, clay contents and salinity (cf. Choudhury et al., 2001), the inversion results of DC resistivity soundings have to be correlated with subsurface geological information.

Quantitative interpretation of DCR field data was carried out to obtain the true resistivity and thickness of subsurface layers by using *ZondIP1D* software version 5.1 (Kaminskiy, 2014). It is based on linear filtering as 1D forward modeling, the Newton algorithm of the least number of layers solves the inverse problem. A preliminary 1D model (thickness and resistivity) can be used for regularizing the process of fitting error minimization. An important advantage of this program is that the data for a profile are treated as a unit representing the geological structure of the survey area as a whole. The interpretation of DCR soundings has been inspected to recognize the number of geoelectrical layers, their depth, thickness and their resistivity. This helps to obtain lateral and vertical extensions of the major geological units.

The obtained results of DCR soundings interpretation are used to visualize the horizontal and vertical variations at the surveyed area; the interpreted resistivity values with depths at all sounding points were used to create a 3D slicing model. The 3D visualization model was computed using the inverse distance-anisotropic algorithm of the Rockworks software package (RockWare, 2017). Additionally, five locations were selected for 2D resistivity surveys according to the results deduced from the DCR soundings. The Wenner-Beta configuration was used to estimate the apparent resistivity of the underlying sediments. The length of the profiles ranged between 52 m and 172 m and were measured using 26 to 44 electrodes with electrode spacing of 4 m (ERT_1 and ERT_2) and 2 m (ERT_3, ERT_4 and ERT_5) for maximum factors (n) equal to seven (see Fig. 2; Table 1). The different electrode spacing caused different penetration depths and resolutions. The electrode spacing was selected according to the results deduced from the DCR soundings and the available boreholes. The electrode locations at the start and end of a profile were documented using a standard GPS device (Garmin GPSMAP 60CSx). The differences in terrain surface elevation were of minor relevance due to the rather flat terrain; nevertheless, they were noted manually.

Table 1
Name, length, electrode spacing and drilling location of 2D ERT profiles.

Profile	Length [m]	Electrode spacing [m]	Drilling location
ERT_1	172	4	Z1, Z2
ERT_2	112	4	Z4
ERT_3	52	2	Z4
ERT_4	64	2	Z3
ERT_5	52	2	Z5

The 2D resistivity profiles were inverted using RES2DINV x64 ver. 4.08 (Geotomo, 2017). This program is based on the smoothness constrained least squares inversion algorithm (de-Groot-Hedlin and Constable, 1990) and was developed by Loke and Barker (1995, 1996) to produce fast inversion procedures for 2D resistivity. Five iterations were used to generate the 2D profiles. The Root Mean Square Error (RMS) was between 2.3% and 5.5% for the profiles ERT_1, ERT_2, ERT_3, ERT_4 and ERT_5, which are presented in the results section of this manuscript. The 2D resistivity inversion aims to construct an image of the obtained true subsurface resistivity distributions along the measured profiles.

4. Results

4.1. Geomorphological investigations

Fig. 3 provides a panoramic overview of drilling locations (2016 & 2018) and shows examples of the recovered sediments. The results of the drilling campaign in 2016 are presented in more detail in Ullmann et al., 2019, while the main findings from the geomorphological investigations in 2016 and 2018 are compiled in Fig. 4, illustrating sedimentary structures, sediment colour, dominating grain sizes and the presence of potsherds and redoximorphic features.

Drillings at Z1 and Z2 were drilled to a maximum depth of approximately three metres. It was not possible to reach sediments lower than 3.25 m asl, as a solid layer was present. Several attempts to break through this layer failed at both locations. After the recovery, the drill head blades showed small limestone fragments. All samples between 6.4 and 3.25 m asl belonged to the surface cover layer, which is a mixture of varying modern and ancient debris of all grain sizes. Hereafter, this layer will be referred to as the “surface layer”.

At location Z3, the drilling reached a maximum depth of approximately seven metres, which was also the maximum depth attainable by the given equipment. It was possible to penetrate the surface layer, which noticeably showed a thin layer of silty and clayey material between 4.2 and 3.7 m asl. From 2.2 to 0.9 m asl, a massive layer consisting of silt and clay was observed (see Fig. 3f). The sediments were dark brownish to greyish in colour and the soil moisture was significantly higher than in the overlying layer. The deposits contained many small ceramic and charcoal fragments. Unfortunately, all pottery fragments were too small to be dated with any certainty, which is also true for the following samples. Some sediment sequences showed a parallel lamination, while grain sizes varied only slightly. A sharp boundary at 0.9 m asl separates this material from the underlying sediments.

The sediment deposits between 0.9 and −1.05 m asl were characterized by alternating sequences of silty/clayey and sandy material, which were horizontally layered and contained many potsherd and charcoal fragments. The soil moisture was high and redoximorphic features were observed from −0.1 m asl onwards. The sediment colours ranged from brownish to greyish. Another fairly sharp planar boundary was present at −1.05 m asl. The underlying layer (−1.05 to −1.35 m asl) was dominated by silty/clayey material of dark colour, showing

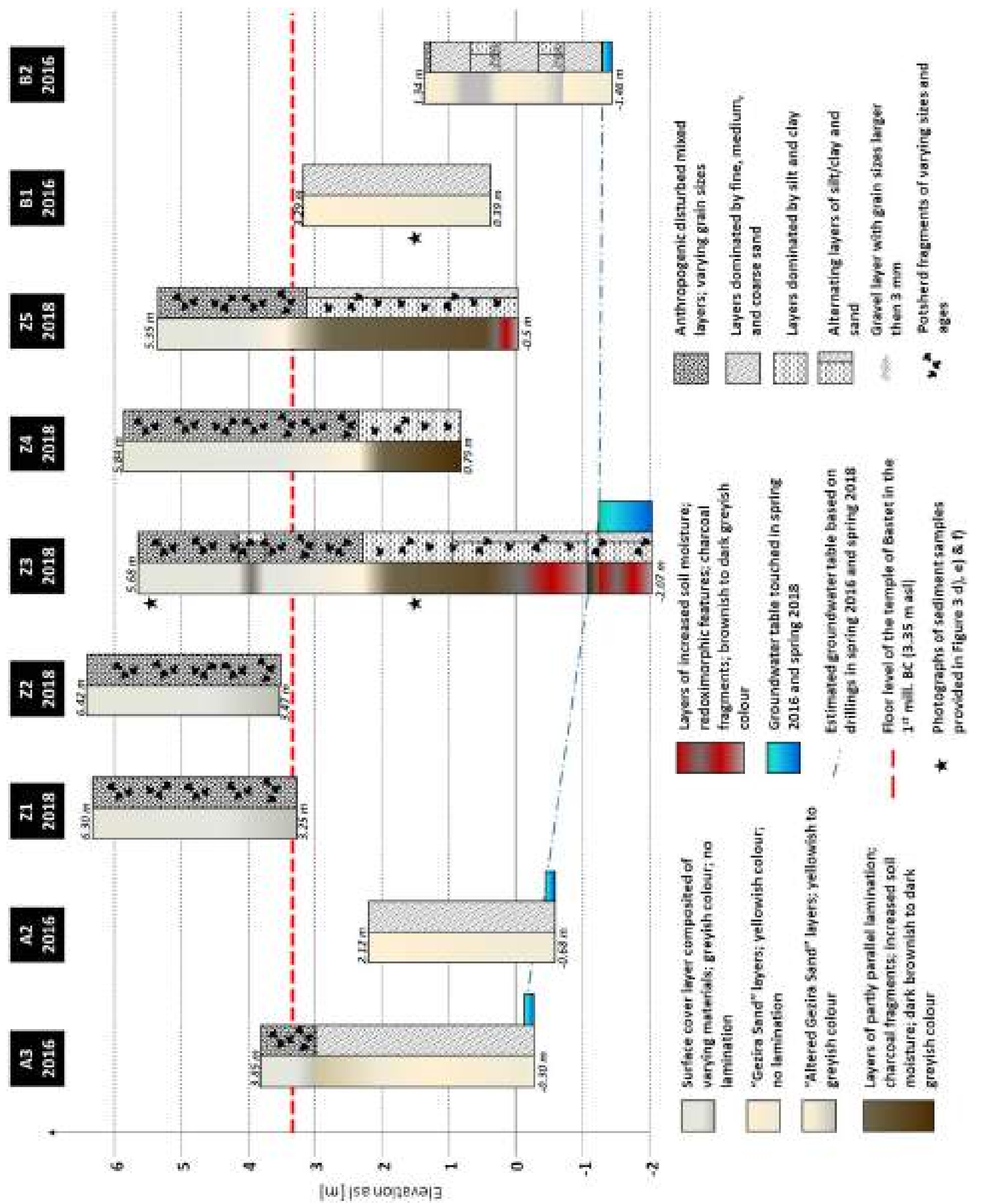

Fig. 4. Generalized results of drilling and sediment analyses in spring 2016 and spring 2018. The drilling locations are indicated in Fig. 2. Drilling was conducted using the Edelman Equipment and the sediment records represent mixed samples. Pictures of samples of "Surface Layer", "Gezira Sand" and "Silt and Clay Layer" are provided in Fig. 3d), e) and f).

redoximorphic features. Also, many small ceramic and charcoal fragments occurred. Below −1.35 m asl, the groundwater table was touched and redoximorphic features were frequently observed. In this lowermost section, sediments were generally brighter in colour and showed alternating sequences of clayey, silty and fine sandy deposits.

Location Z4 is situated at a distance of approximately 20 m from location Z3. The drilling started nearly at the same terrain surface elevation as at location Z3 and reached a depth of approximately five metres. The surface layer was present between 5.84 and 2.2 m asl. Similar to the drilling core Z3, there was a massive dark layer of silt and clay that ranged from 2.2 m asl to the final depth of the coring at 0.79 m asl. Compared to the samples of Z3, the sediments of Z4 were overall very similar but had a higher silt content. All samples of Z4 contained pottery fragments, which were usually larger than those of Z3.

Location Z5 was situated further north between the Temple of Bastet and the museum. The distance to boreholes Z3 and Z4 was approximately 70 m. The surface layer was present between 5.25 and 3.2 m asl. Deposits below this depth were finer in texture and darker in colour, showing several alternations of silty/clayey and sandy sediment sequences. All layers contained potsherd fragments that were usually larger than the ones observed in Z4.

Some of the anthropogenic artefacts were cement fragments, likely of Roman date as could be observed by its typical manufacture. Similar pieces were attested in remains of Roman architecture in the nearby area during the archaeological survey of the Tell. From about 0.3 m asl onwards redoximorphic features were present.

4.2. DCR soundings

Along with the drillings, DCR soundings and 2D ERT measurements were conducted. Fig. 5 shows an example of the results of DCR sounding at location Z3 and highlights the relation between the drilling records and the subsurface resistivity. Preliminary consideration of the inversion results of DCR soundings together with the correlation of the geoelectrical horizons and the lithology of the available boreholes allows a resistivity spectrum for the subsurface layer distribution to be established. Comparing the sedimentary record and the resistivity values, the dark layers dominated by silt and clay are characterized by lower values (10 Ωm) in the 1D measurement. In contrast, the surface layer is characterized by high resistivity values of about 150 Ωm. Between 0.5 and 1.5 m below the terrain surface low resistivity values of about 8 Ωm were observed, which can be linked to a thin layer of silty/clayey deposits at the same depth (see above). Fig. 5 shows the high correlation between the calculated apparent resistivity values from 2D inversion and the measured data from the DC sounding. The model shows the main two geoelectrical layers comprising a low resistivity layer with resistivity < 10 Ωm and a thickness of about 2 to 7 m overlying a high resistivity layer with resistivity values of > 10 Ωm.

A 3D view of E-W cross sections with slicing at different depths was carried out to understand the lateral and vertical extension of the revealed subsurface resistivity (Fig. 6). The resistivity slice maps indicated a trough-like, linear structure of low subsurface resistivity values between the Temple of Bastet and the museum, whereas layers under the museum and the temple were characterized by layers of higher resistivity (Fig. 6). The layer extends nearly 7 m in depth.

4.3. ERT profiles

Confirmation of the above results came from the 2D ERT profiling presented in Fig. 7 for the five profiles ERT_1 to ERT_5. The inversions were processed using five iterations and the sections are drawn with the same colour bar. ERT_1 (Fig. 7a) showed higher resistivity values in the first half of the profile in a northwestern direction towards the museum. The resistivities underneath location Z1/Z2 were comparably high and ranged from 47 to 95 Ωm. The second half of the profile in a southeastern direction towards the eastern tell was characterized by two units: first, a layer near the surface with high resistivity values (> 300 Ωm); second, a layer of low resistivity values (< 24 Ωm) underneath that surface layer. ERT_2 (Fig. 7 b) showed higher resistivity values, mostly larger than 47 Ωm, in a northwestern direction towards the museum and lower resistivity values (< 47 Ωm) in a southeastern direction towards the eastern tell. The southern part of the profile showed

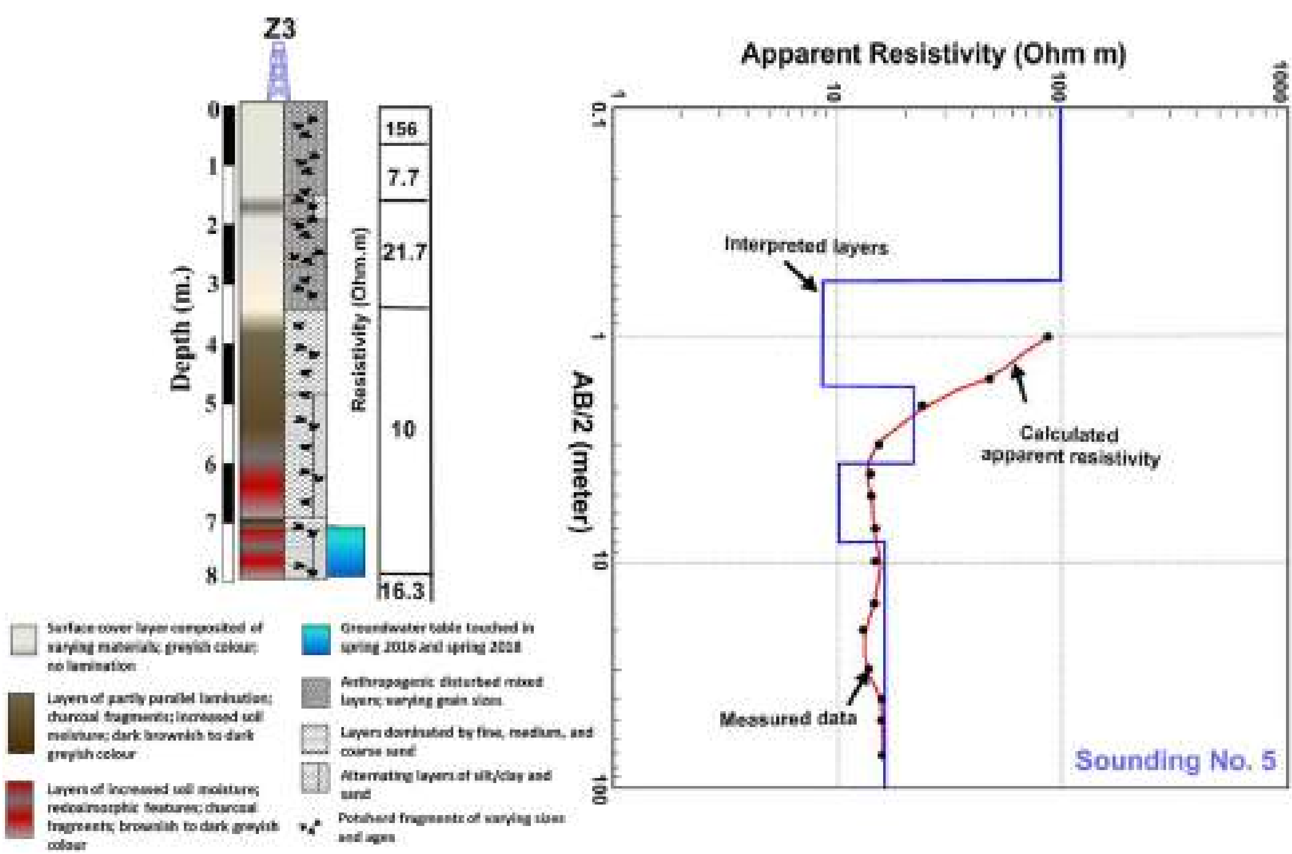

Fig. 5. Example of DCR sounding point No. 5 located at drilling location Z3: generalized records from sediment analyses and the apparent resistivity values from 1D DC sounding (left); plot of calculated apparent resistivity values (from 2D inversion) versus 1D measured data and interpreted layers (right).

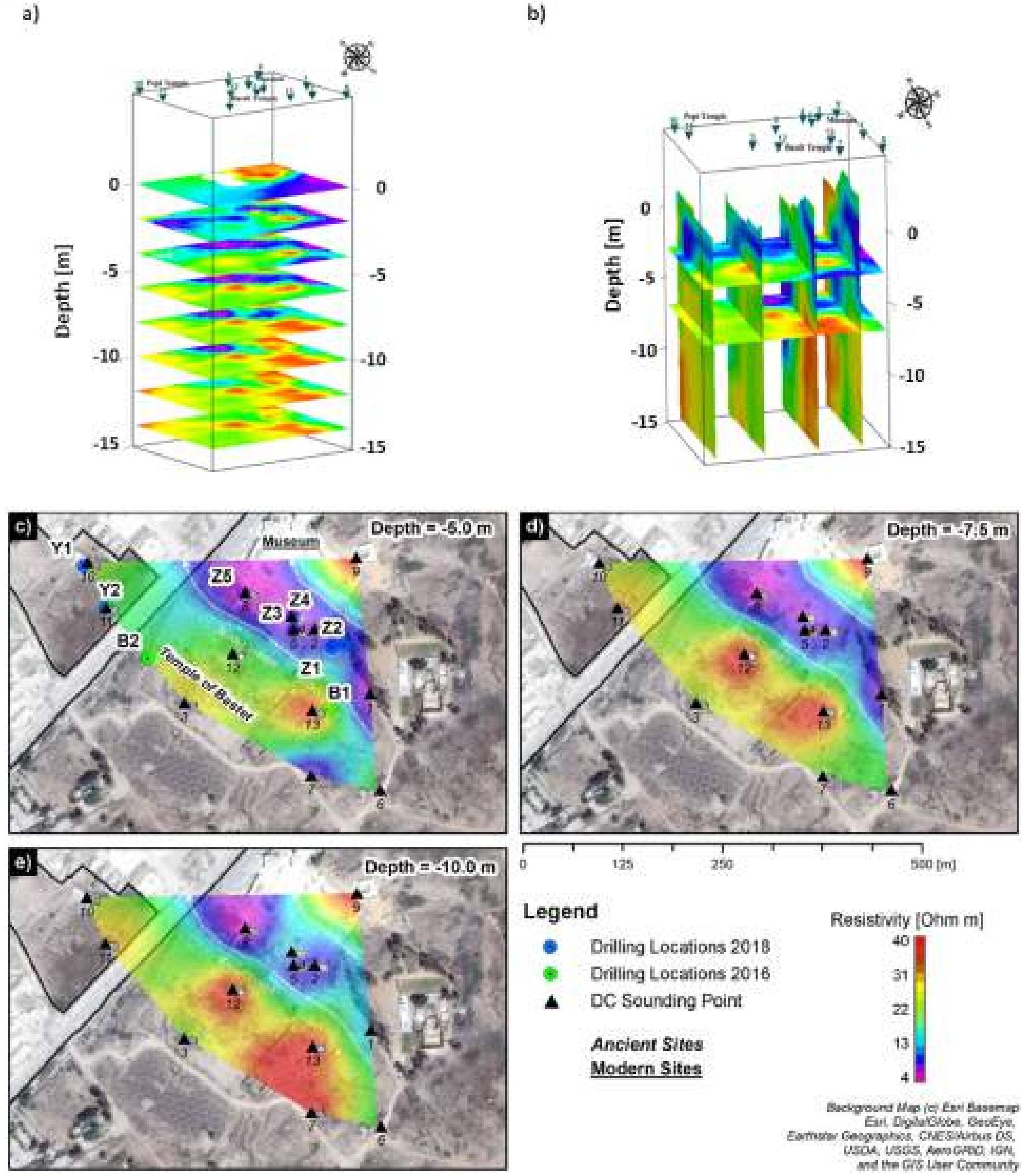

Fig. 6. Resistivity slice maps interpolated using all thirteen DCR sounding points. Maps show interpolated subsurface resistivities: a) maps with horizontal slices showing the resistivity distribution at different depths; b) 3D view of W–E cross sections with horizontal slices showing the lateral and vertical variation of resistivity; selected horizontal slices at estimated depths of c) −5.0 m, d) −7.5 m and e) −10.0 m below the terrain surface. The white dashed lines indicate the potential track of the waterway and follow approx. the 10 Ωm isoline.

a trough of very low resistivity values (< 24 Ωm) and was covered by layers near the surface of higher resistivity values (> 24 Ωm). The drilling location of Z4 was situated between the northern and southern part of the profile. ERT_3 (Fig. 7 c) was oriented in a southwestern to northeastern direction and creates a section between the Temple of Bastet (south) and the museum (north). The surface layer was characterized by higher resistivity values (> 47 Ωm) and the thickness of this layer increased towards the Temple of Bastet. Underneath this layer, lower resistivity values (< 24 Ωm) were present. Similarly, ERT_4 (Fig. 7d) showed a surface layer that was characterized by higher resistivity values (> 47 Ωm) while underneath this layer, lower resistivities (< 12 Ωm) were present. ERT_5 (Fig. 7e) provides a section between the Temple of Bastet and the museum and was oriented in a southwestern to northeastern direction. The first part of the profile was

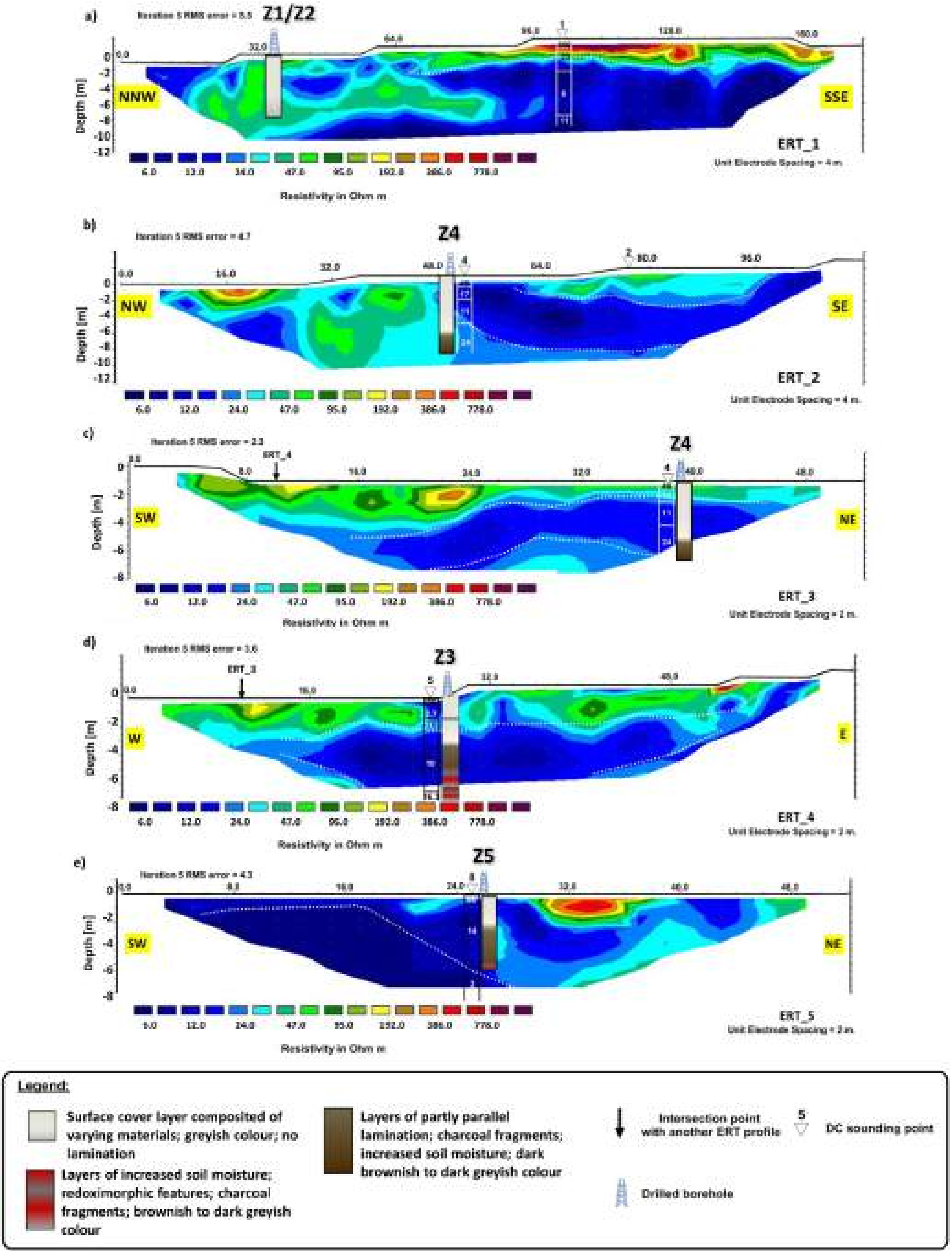

(caption on next page)

Fig. 7. 2D Electrical Resistivity Tomography (ERT) Profiles of drilling locations (Z1, Z2, Z3, Z4, Z5): a) ERT Profile 1 located parallel to the northern side of the Temple of Bastet, b) ERT Profile 2 located between the northern border of the Temple of Bastet and the site museum, c)-e) ERT Profiles 3, 4, and 5 located between the northern border of the Temple of Bastet and the site museum (cross profiles). White triangles indicate the locations of 1D DC soundings and numbers display the measured resistivity in Ωm.

characterized by very low resistivity values (< 12 Ωm), while the second part was characterized by higher values (> 12 Ωm). The borehole location Z5 was situated between the northern and southern part of the profile. The results obtained from the 2D ERT surveys are well in concordance with the results of DCR soundings and the information from the drilled boreholes.

5. Discussion

The drilling campaign in 2018 revealed clayey/silty deposits at depths below 2.5 m asl between the Temple of Bastet and the site museum, below the floor level of the Temple of Bastet of the 1st mill. BCE (3.35 m asl). This fine-grained material along with its dark colour, suggesting an increased content of organic matter, indicates a stillwater facies that must have been accumulated in a body of water with very low flow velocity. Ginau et al. (2018) have presented drilling records on canal infills in the Western Nile Delta and categorized these sediments as deposits of a low energy system that are characterized by fine-grained materials, rich in organic matter, with homogeneous intercalations. Similarly, Brown (1997) noted that paleo-canals and cut-offs are typically infilled with sediments of finer grain sizes (silt/clay) and organic matter, i.e. peat. Naturally, such features can be formed by the abandonment of former river channels, ox-bow lakes or neck cut-offs (Brown, 1997; Toonen et al., 2012). In contrast, sediments of high-energy systems, such as natural rivers, usually exhibit coarser grain sizes, depleted content of organic matter, and heterogeneous intercalations with alterations in grain size linked to graded sequences (Brown, 1997; Ginau et al., 2018).

The recovered clay and silt dominated sediments at Bubastis fit the above-mentioned concept of a low energy system. It is therefore likely that the sediments described represent infills of a former waterway or water body. This fluvial or limnic system must in turn have had a connection to a headwater for a longer period, as it was situated in the central part of the Tell and deposited sediments were at least four metres thick. The identified laminations may therefore indicate changes in the water supply of the headwater, i.e. due to Nile floods, or changes in the water management system. The observation of very fine-grained sediments and the absence of medium and fine sands in the upper part of Z3 indicate that this clay-rich layer represented the last period of the waterway just before it was silted up and buried by the debris of the following epochs. The sediments below that layer (0.9 to −1.35 m asl) were similar but coarser in texture, i.e., fine to medium sands were present. Due to the alternation of clayey/silty and sandy sequences, it is likely that these sediments indicate an earlier, more active phase. However, sediments were still deposited in a fluvial or limnic system with a generally low flow velocity in the sense of Ginau et al. (2018).

The difference to the succeeding phase is the existence of a stable connection to a headwater. As mentioned in the preceding section, the varying contents of silt, clay and sand may be explained by changes in the water supply of the headwater due to the annual Nile floods; finer grain sizes indicate periods of low flow velocity and coarser grain sizes indicate periods of higher flow velocity. Therefore, the connection to the headwater at this stage must have been intact and uninterrupted.

ERT surveying was carried out in 2018 in addition to the geomorphological investigations in order to extrapolate the results of sediment analyses to a larger area, i.e. to find evidence of the former course of the waterway. Bubastis is located on the very fringes of the central Delta sand shield (Butzer, 1976) and on lower ground, closer to the groundwater (Ullmann et al., 2019). Therefore, the ERT surveying faces the problem that the influence of the groundwater may blur differences in the sediments' resistivity, e.g., the presence of groundwater favors lower resistivities, as water has a higher electrical conductivity (Tellford et al., 1990; Reynolds, 2011). The results from drilling indicated the groundwater table at a level of about −1.2 m asl, which means that the resistivities of the upper seven metres of the ERT profiles (Fig. 7) are not influenced by groundwater. In turn, profiles ERT_3, ERT_4, and ERT_5 should not be affected by the groundwater, as these profiles display maximum depths of seven metres below the terrain surface. On the contrary, the influence of the groundwater was visible in profile ERT_1, where resistivities between 7 and 11 m below the terrain surface were very low (< 12 Ωm) throughout the section. The observed anomalies were therefore most likely caused by stratigraphic differences, as indicated by the DC soundings, showing a good correlation between observed differences in grain size and subsurface resistivity. The clay-rich layers were characterized by lower resistivities, whereas layers of coarser texture were characterized by higher resistivities. The results of the ERT surveying and DCR sounding are therefore in line with the observations from the sediment analyses. The surface layer (low soil moisture; varying grain sizes with low contents of silt/clay) of the upper three to four metres was usually shown in the ERT profiles with higher resistivity values, whereas the underlying clayey/silty deposits were characterized by lower resistivity values (this is most visible for location Z3 in Fig. 7d and location Z4 in Fig. 7c). We may therefore conclude that profiles ERT_2 and ERT_3 show cross sections and that profile ERT_4 shows a longitudinal section of the buried waterway between the northern border of the Temple of Bastet and the museum. This observation is in agreement with the resistivity slice maps that were interpolated using all thirteen DC soundings points (Fig. 6).

Based on the results of the ERT modeling and the drilling campaigns, we suggest that locations Z3, Z4 and Z5 were situated at different positions on a buried waterway. Among the drillings of Z3, Z4 and Z5, it was observed that the sediments and potsherd fragments of Z3 were smaller in grain size than the ones of Z4; while the sediments and potsherd fragments of Z4 were finer than those of Z5. Therefore, it seems likely that Z3 was potentially located in a more central position, while Z4 and Z5 were possibly located closer to the bank or shore. Additionally, Z5 was presumptively in closer proximity to the tributary than Z4 and Z3. This might explain the decrease in the dominating grain size from Z5 to Z3 and would be in line with the results from ERT surveying. Taking this further, the location of the headwater would then have been north or northwest of the Temples of Bastet and Pepi I. Regardless of this interpretation, the presence of fine-grained material indicates a fluvial or limnic deposition history in an overall low energy system (Ginau et al., 2018). This observation is corroborated by the absence of coarse sand and pebbles, which signifies a low flow velocity. The system was potentially a cut-off, ox-bow lake or a dead stream branch of the actual channel network (Brown, 1997).

The ERT surveying indicates a waterway width of about 20 to 30 m (which matches the description of Herodotus); however, the orientation of this waterway cannot be determined exactly, and the said width is a preliminary estimate. The results of ERT_1 and the slice maps of the DCR soundings suggest that the system was located between the Temple of Bastet and the site museum and continued eastward; however, layers of higher electrical resistivity bordered it in the north (site museum) and south (Temple of Bastet). This, in turn, might be caused by the existence of Gezira sands that were previously reported by Ullmann et al., 2019 for these locations. This interpretation is supported by the presence of pottery fragments: all sediment deposits of Z3-Z5 contained ceramic fragments below the floor level of the Temple of Bastet. In contrast, the sediments that were recovered from the same depths in 2016 underneath the Temple of Bastet, Cemetery A, and the Middle Kingdom Palace did not contain any ceramic fragments. The small potsherds found in 2018 most probably cover all historical periods of human occupation of the city and suggest the presence of the waterway throughout these epochs; however, it was not possible to date the potsherds, as they did not show any diagnostic features that would allow certain dating. Moreover, radiocarbon dating of the charcoal pieces has not been carried out yet, although it is planned for future investigations. At location Z5, fragments of Roman cement came to light, which suggests that the waterway was not silted up in the Roman period, i.e. it is likely that the system was bearing water in the 5th century BCE, meaning Herodotus might have actually seen it, as it is a terminus post quem.

Overall, it is striking that the clayey/silty deposits were found in the most central part of the Tell. As mentioned in the preceding section, the recovered sediments from drillings Z3 and B1 below 1.5 m asl showed very different compositions and colours ("Gezira sands"), even though both were recovered from the central area of the site, from the same depth, and in close proximity to each other. These findings make it likely that the waterway separated the temple district from the area of the cemeteries. Still, it remains unclear how the system was related to its feeding ancient Nile branch and where the latter was actually located. So far, it is only certain that there must have been a tributary that allowed infilling and refilling. As discussed above, Herodotus reported a second, corresponding canal at the southern side of the Temple of Bastet, which sprang from the same Nile branch, but this canal so far remains undiscovered.

All in all, drawing on Herodotus' description, which nevertheless should still be treated with caution, it seems most likely that said tributary was situated north of the Temple of Bastet, as Herodotus mentioned that both canals were connected to the Nile but did not meet ["(…) *for channels come in from the Nile, not joining one another, but each extending as far as the entrance of the temple, one flowing round on the one side and the other on the other side*"]. This would make it seem possible that a feeder canal connected the temple canals with the Nile branch.

The feeder canal was then either situated between the Temple of Pepi I and the Temple of Bastet, or north of the Temple of Pepi I. Judging from the sedimentary records of drilling location B2 at the western side of the Temple of Bastet (Fig. 2), which showed fluvial sediments composed of coarse sand and large pebbles, the connecting point of the tributary and the Nile would presumptively be located west or northwest of the Temple of Bastet and/or the Temple of Pepi I. However, this is a working hypothesis that will require more investigation for its verification. The missing dating especially limits the interpretation and correlation of the sediment records as no chronostratification of the sediments exists so far.

6. Conclusions

Geomorphological and geophysical investigations were undertaken at the excavation site of Bubastis, located in the Eastern Nile Delta close to the city of Zagazig, in order to find evidence of the existence and location of the sacred canals of Bubastis, as were described by Herodotus in the 5th century BCE. Preceding archaeological missions had not discovered remains of these canals.

Drilling and sediment analyses in 2018 revealed fine-grained sediments in the central area of the site at depths below 2.5 m asl between the Temple of Bastet and the site museum, which were situated below the floor level of the Temple of Bastet (1st millennium BCE) at 3.35 m asl. The recovered sediments were silty/clayey in texture and rich in ceramic fragments. They are interpreted as fluvial or limnic deposits that were accumulated in a low energy regime, characterized by low flow velocities. In addition, the waterway must have had a connection to a headwater for a longer period, as it was situated in the central part of the Tell and sediment deposits were at least four metres thick. The alternation of clayey, silty and sandy sequences may therefore be a result of changes in the water supply of the headwater. The results of DCR soundings and 2D Electrical Resistivity Tomography surveying indicated trench-like layers of low resistivity values between the Temple of Bastet and the site museum and were in line with the results of the geomorphological investigations. Additionally, layers of high resistivity values were found under the Temple of Bastet and the museum, supporting the findings of Ullmann et al. (2019) by indicating the local extent of the Gezira mound.

Combining the results of both methods, it seems likely that the discovered facies belonged to the ancient waterway that was described by Herodotus as one of the canals of Bubastis. Presumably, this waterway was fed by a tributary that was situated north or northwest of the Temples of Bastet and Pepi I. However, the sediment analyses were performed on site only, and it has not yet been possible to conduct further laboratory analyses or date the recovered pottery or charcoal fragments. This limits the interpretation and correlation of the sediment records. Nevertheless, the possible detection of the existence and course of the northern part of the sacred canals, the *Isheru* of the ancient Egyptian texts, which once surrounded the Temple of Bastet at Bubastis, is highly relevant: for the first time, we now possess more than written accounts of their existence. Future investigations will focus on the relation of the discovered waterway to the temples, palaces, cemeteries and the settlement zones of Bubastis and on how the system was connected to the Nile with regard to the longer landscape history. Moreover, as the locations and activities of Nile branches and smaller water canals caused the flourishing and decline of settlements, the geoarchaeological research conducted at the canals of Bubastis will further understanding of the human-environment relation in the Nile Delta in general.

Funding sources

This work was supported by the University of Würzburg "*Forschungsfond der Philosophischen Fakultät* (*2018-2020*): *Die Sakrallandschaft von Bubastis*: *Geoarchäologische Untersuchungen zu den heiligen Wasserkanälen des Tempels der Bastet*"; Gerda Henkel Stiftung (2016–2018) "*Der Tempelbezirk der 6. Dynastie in Tell Basta*: *Eine Fallstudie zur Rolle der Provinztempel bei der Herausbildung städtischer Zentren im Nildelta im 3. Jt. v. Chr.* (*AZ 41/V/17*)". The funders had no role in the design of the study; in the collection, analyses, or interpretation of data; in the writing of the manuscript; or in the decision to publish the results. This publication was funded by the German Research Foundation (DFG) and the University of Würzburg in the funding program Open Access Publishing.

Acknowledgments

The authors would like to thank Dr. Christian Büdel (University of Würzburg) and Prof. Tian Gang (Zhejiang University, China) for the helpful discussions on the interpretation of the results. The Digital Elevation Model of the TanDEM-X Mission is shown with the permission of the German Aerospace Center (DLR), related proposal; "*DEM_HYDR1426 - Geoarcheology of the Nile delta, an integrated research collaboration of the University of Würzburg and University of Frankfurt that seeks to deduce geomorpholocial and palaeoenvironmental information from Tandem-X DEM data*" (Principal Investigators: A. Ginau, R. Schiestl, J. Wunderlich, E. Lange, T. Ullmann). We acknowledge the use of imagery from the Worldview Snapshots application (https://wvs.earthdata.nasa.gov/), part of the Earth Observing System Data and Information System (EOSDIS). We thank the reviewers for their constructive and helpful comments and Dr. Katharine Thomas for proofreading of the manuscript.

References

Ad-hoc-Arbeitsgruppe Boden (BKA), 2005. Bodenkundliche Kartieranleitung. H. Sponagel; W. Grottenthaler; K.-J. Hartmann; R. Hartwich; P. Janetzko; H. Joisten; D. Kühn (Red.) In: Eckelmann, Wolf (Ed.), Bundesanstalt für Geowissenschaften und Rohstoffe in Zusammenarbeit mit den Staatlichen Geologischen Diensten; K.-J. Sabel; R. Traidl (Hrsg.), Ad-hoc-Arbeitsgruppe Boden. 5. verbesserte u. erweiterte Auflage, (438 pp).

Arnold, D., 1992. Die Tempel Ägyptens: Götterwohnungen, Kultstätten, Baudenkmäler. Artemis & Winkler, Zürich.

Assmann, J., 1984. Ägypten: Theologie und Frömmigkeit einer frühen Hochkultur. Urban-Taschenbücher 366 Kohlhammer, Stuttgart.

Bakr, M.I., Lange, E., 2016. Die Nekropolen des Alten Reiches in Bubastis. In: Feder, F., Sperveslage, G. (Eds.), Gedenkschrift für Erika Endesfelder, Internet - Beiträge zur Ägyptologie und Sudanarchäologie XVIII, pp. 31–48 (London).

Bates, R., Martin, C., Richard, B., Whittaker, E.J., 2007. Mixed method approaches to the investigation and mapping of buried quaternary deposits: examples from southern England. J. Archaeological Prospection 14 (2), 104–129.

Bevan, B.W., Roosevelt, A.C., 2003. Geophysical exploration of Guajara` a prehistoric earth mound in Brazil. J. Geoarchaeology 18 (3), 287–331.

Bietak, M., 1975. Tell el-Dab'a II, Der Fundort im Rahmen einer archäologisch-geographischen Untersuchung über das ägyptische Ostdelta. Untersuchungen der Zweigstelle Kairo des Österreichischen Archäologischen Instituts 1, Wien.

Bietak, M., Lange, E., 2014. Tell Basta: the palace of the middle kingdom. Egyptian Archaeology 44, 4–7.

Brissaud, P., 2018. Tanis, le domaine de la déesse Mout et son lac sacré. BoD – Books on Demand, Norderstedt, Allemagne, pp. 184.

Brown, A.G., 1997. Alluvial Geoarchaeology. Floodplain Archaeology and Environmental Change. Cambridge University Press, pp. 401.

Bussmann, R., 2010. Die Provinztempel Ägyptens von der 0. bis zur 11. Dynastie, Probleme der Ägyptologie 30, 2010. Brill, Leiden.

Butzer, K., 1959. Studien zum vor- und frühgeschichtlichen Landschaftswandel der Sahara III: Die Naturlandschaft Ägyptens während der Vorgeschichte und der dynastischen Zeit. Akademie der Wissenschaften und der Literatur: Abhandlungen der Mathematisch-Naturwissenschaftlichen Klasse. Wiesbaden: Akademie der Wissenschaften und der Literatur in Mainz (2), 71–78.

Butzer, K.W., 1976. Early hydraulic civilization in Egypt: A study in cultural ecology. In: Prehistoric Archeology and Ecology. The University of Chicago Press, Chicago; London, pp. 149.

Butzer, K.W., 2002. Geoarchaeological implications of recent research in the Nile Delta. In: van den Brink, E.C.M., Levy, Th.E. (Eds.), Egypt and the Levant: Interrelations from the 4th through the Early 3rd Millennium BCE. Leicester University Press, London; New York, pp. 83–97.

Choudhury, K., Saha, D.K., Chakraborty, P., 2001. Geophysical study of saline water intrusion in a coastal alluvial terrain. J. Appl. Geophys. 46, 189–200.

Deiana, R., Bonetto, J., Mazzariol, A., 2018. Integrated electrical resistivity tomography and ground penetrating radar measurements applied to tomb detection. Surv. Geophys. 39, 1081–1105. https://doi.org/10.1007/s10712-018-9495-x.

El-Kenawy, A., Metwaly, M., Gemail, Kh., Abd El-Raouf, A., 2013. Contribution of geoelectrical resistivity sounding for paleoenvironment assessment at Saft El-Henna and Tell El-Dab'a archaeological sites, eastern Nile Delta, Egypt. Explor. Geophys. 44 (4), 282–288.

El-Sawi, 1979. Excavations at Tell Basta. Reports of Seasons 1967–1971 and Catalogue of Finds. Charles University of Prague.

Farid, S., 1964. Preliminary report on the excavations of the antiquities Department at Tell Basta (season 1961). Annales du Service des Antiquités de l'Egypte 58, 85–98.

Food and Agriculture Organization of the United Nations (FAO), 2015. World reference base for soil resources 2014. International soil classification system for naming soils and creating legends for soil maps - update 2015. World Soil Resources Reports 203.

Geotomo Software, 2017. RES2DINV - Manual. https://www.geotomosoft.com/, Accessed date: 5 December 2018.

Gessler-Löhr, B., 1983. Die heiligen Seen ägyptischer Tempel: ein Beitrag zur Deutung sakraler Baukunst im alten Ägypten, Hildesheimer Ägyptologische Beiträge 21, 1983. Gerstenberg, Hildesheim.

Ginau, A., Schiestl, R., Wunderlich, J., 2018. Integrative geoarchaeological research on settlement patterns in the dynamic landscape of the northwestern Nile delta. Quat. Int. JQI 7409 (*in press*).

de-Groot-Hedlin, C., Constable, S.C., 1990. Occam's inversion to generate smooth two dimensional models from magnetotelluric data. Geophysics 55, 1613–1624.

Habachi, L., 1957. Tell Basta, Supplément Annales du Service des Antiquités de l'Egypte 22. Imprimerie de l'Institut français d'archéologie orientale, Le Caire.

Kaminskiy, A.E., 2014. ZONDIP1D Version 5.1, Program for One-Dimensional Interpretation of Data Obtained by VES and VES-IP (Ground and Marine Measurements), User's Manual. Zond geophysical software, Saint-Petersburg (68 p).

Kasprzak, M., Traczyk, A., 2014. LiDAR and 2D electrical resistivity tomography as a supplement of geomorphological investigations in urban areas: a case study from the City of Wrocław (SW Poland). Pure Appl. Geophys. 171, 835–855. https://doi.org/10.1007/s00024-013-0693-7.

Kitchen, K., 1996. The Third Intermediate Period in Egypt (1100–650 B.C.), 2nd ed. (Warminster).

Lange, E., 2006. Die Ka-Anlage Pepis I. in Bubastis im Kontext königlicher Ka-Anlagen des Alten Reiches. Zeitschrift für Ägyptische Sprache und Kultur 133, 121–149.

Lange, E., 2008. Legitimation und Herrschaft in der Libyerzeit: eine neue Inschrift Osorkons I. aus Bubastis (Tell Basta). Zeitschrift für Ägyptische Sprache und Kultur 135, 131–141.

Lange, E., 2009. The Sed-festival reliefs of Osorkon II at Bubastis: New investigations. In: Broekman, G.P.F., Demare, R.J., Kaper, O. (Eds.), The Libyan Period in Egypt. Historical and Cultural Studies into the 21st-24th Dynasties: Proceedings of a Conference at Leiden University, 25–27 October 2007. vol. 23. Egyptologische Uitgaven, pp. 205–220.

Lange, E., 2010. King Shoshenqs of Bubastis, Egyptian. Archaeology 37, 1–3.

Lange, E., 2013. The old kingdom temples and cemeteries of Bubastis. Egyptian Archaeology 42, 8–10.

Lange, E., 2015. The so-called governor's cemetery at Bubastis and provincial elite tombs in the Nile Delta: state and perspective of research. In: Miniaci, G., Grajetzki, W. (Eds.), The World of the Middle Kingdom (2000–1550 BC). Contributions on Archaeology, Art, Religion and Written Sources. vol. 1. pp. 187–203.

Lange, E., Ullmann, T., 2015. Goddess on the water: the sacred landscape of Bubastis. Egyptian Archaeology. EA 47, 17–19.

Lange, E., Ullmann, T., Baumhauer, R., 2016. Remote sensing in the Nile Delta: Spatio-temporal analysis of Bubastis/Tell Basta. Egypt and the Levante - International Journal for Egyptian Archaeology and Related Discipline 26.

Lange-Athinodorou, E., 2019. Der "Tempel des Hermes" und die Pfeile der Bastet: Zur Rekonstruktion der Kultlandschaft von Bubastis. (Festschrift Hans-Werner Fischer-Elfert (*in print*).

Leclère, F., 2008. Les villes de Basse Égypte au Ier millénaire av. J.-C.: analyse archéologique et historique de la topographie urbaine. 2 vols. Bibliothèque d'étude 144 Le Caire: Institut français d'archéologie orientale.

Loke, M.H., Barker, R.D., 1995. Least-squares deconvolution of apparent resistivity pseudosections. Geophysics 60 (6), 1682–1690.

Loke, M.H., Barker, R.D., 1996. Rapid least-squares inversion of apparent resistivity pseudosections by a quasi-Newton method. Geophys. Prospect. 44, 131–152.

Maillet, G., Rizzo, E., Revil, A., Vella, C., 2005. High resolution electrical resistivity tomography (ERT) in a transition zone environment: application for detailed internal architecture and infilling processes study of a Rhoˆ ne River paleo-channel. Mar. Geophys. Res. 26, 317–328. https://doi.org/10.1007/s11001-005-3726-5.

Meeks, D., 2006. Mythes et légendes du Delta d'après le papyrus Brooklyn 47.218.84, Mémoires publiés par les membres de l'Institut français d'archéologie orientale 125, 2006. Institut Français d'Archéologie Orientale, Le Caire.

Montet, P., 1966. Le lac sacré de Tanis. Imprimerie Nationale/Librairie C. Klincksieck, Paris.

Naville, E., 1891. Bubastis (1887–1889). 8 Egypt Exploration Fund.

Nimnate, P., Thitimakorn, T., Choowong, M., Hisada, K., 2017. LiDAR and imaging and locating paleo-channels using geophysical data from meandering system of the Mun River, Khorat Plateau, Northeastern Thailand. Open Geosci. 9, 675–688.

Patella, D., Hesse, D.A., 1999. Electric, magnetic and electromagnetic methods applied to cultural heritage. J. Appl. Geophys. 41, 135–311.

Pennington, B.T., Sturt, F., Wilson, P., Rowland, J., Brown, A.G., 2017. The fluvial evolution of the Holocene Nile Delta. Quat. Sci. Rev. 170, 212–231.

Reynolds, J.M., 2011. An Introduction to Applied and Environmental Geophysics, 2nd edition. Wiley, pp. 712.

RockWare, 2017. Rockworks geological modeling software. https://www.rockware.com/, Accessed date: 5 December 2018.

Rowland, J., Strutt, K.D., 2011. Geophysical survey and sub-surface investigations at Quesna and Kom el-Ahmar (Minuf), governorate of Minufiyeh: An integrated strategy for mapping and understanding sub-surface remains of mortuary, sacred and domestic contexts. In: Proceedings of the International Conference "Achievements and Problems of Modern Egyptology", Moscow, Russia, September 29–October 2, 2009, pp. 332–349.

Said, R., 1981. The Geological Evolution of the River Nile. Heidelberg, Berlin, New York.

Said, R., 1993. The River Nile. In: Geology, Hydrology and Utilization, (Burlington).

Sauneron, S., 1963-64. Les inscriptions ptolemaïques du temple de Mout à Karnak. Bulletin de l'Institut d'Égypte 45 (1963–64), 45–52.

Sauneron, S., 1983. Villes et légendes d'Égypte, 2nd revised ed. Bibliothèque d'étude 90 Institut français d'archéologie orientale, Le Caire.

van Siclen, C., 1991. The mayors of Basta in the middle kingdom. In: Akten des vierten internationalen Ägyptologen Kongresses, München 1985, pp. 187–194 (Beiheft, Studien zur Altägyptischen Kultur 4.4).

Simms, J.E., Albertson, P.E., 2000. Multidiscipline investigation to locate the Kentucky shipwreck. J. Geoarchaeology 15 (5), 441–468.

Tellford, W.M., Geldart, L.P., Sheriff, R.E., 1990. Applied Geophysics, 2nd edition. Cambridge University Press, pp. 790.

Tillier, A., 2010. Notes sur l'*icherou*. In: Égypte Nilotique et Méditerranéenne. 3. pp. 167–176.

Toonen, W.H.J., Kleinhans, M.G., Cohen, K.M., 2012. Sedimentary architecture of abandoned channel fills. Earth Surf. Process. Landf. 37, 459–472.

Toonen, W.H.J., Graham, Angus, Pennington, Benjamin T., Hunter, Morag A., Strutt, Kristian D., Barker, Dominic S., Masson-Berghoff, Aurélia, Emery, Virginia L., 2017. Holocene fluvial history of the Nile's west bank at ancient Thebes, Luxor, Egypt, and its relation with cultural dynamics and basin-wide hydroclimatic variability. Geoarchaeology 33 (3), 273–290.

Torrese, P., Rainone, M., Colantonio, F., Signanini, P., 2013. Identification and investigation of shallow paleochannels in the chamelecon valley (Honduras): 1d vs 2d electrical resistivity surveys. In: Symposium on the Application of Geophysics to Engineering and Environmental Problems, pp. 321–331. https://doi.org/10.4133/sageep2013-112.1.

Ullmann, Tobias, Lange-Athinodorou, Eva, Göbel, Alexander, Büdel, Christian, Baumhauer, Roland, 2019. Preliminary results on the paleo-landscape of Tell Basta /Bubastis (eastern Nile delta): An integrated approach combining GIS-Based spatial analysis, geophysical and archaeological investigations. Quat. Int. (1040-6182) 511, 185–199. https://doi.org/10.1016/j.quaint.2017.12.053.

Wilkinson, R.H., 2000. The Complete Temples of Ancient Egypt. Thames & Hudson, London.

Wilson, P., 2010. Temple architecture and decorative systems. In: Lloyd, A.B. (Ed.), A Companion to Ancient Egypt 2. Wiley-Blackwell, Chichester; Malden, MA, pp. 781–803.

Yoyotte, J., 1962. Études géographiques, II: les localités méridionales de la région memphite et le "Pehou d'Héracléopolis". Revue d'égyptologie 14 (1962), 75–111.